Label-Free Multimodal Multiphoton Microscopy of Carcinogenesis by Shaping Fiber Supercontinuum Pulses

Stephen A. Boppart, M.D., Ph.D.

Biophotonics Imaging Laboratory
Beckman Institute for Advanced Science and Technology
Departments of Electrical and Computer Engineering, Bioengineering, and Medicine
University of Illinois at Urbana-Champaign

August 20, 2015

Advanced Fluorescence Microscopy Workshop
ISS Fluorescence Foundation

Disclosure

Co-Founder, Chief Medical Officer (Diagnostic Photonics)
Licensing IP from Illinois related to Interferometric Synthetic Aperture Microscopy

Co-Founder, Chief Medical Officer (PhotoniCare)
Licensing IP from Illinois related to optical coherence tomography of the ear and eye

Patent Royalties (MIT – Massachusetts Institute of Technology)
Licensing IP related to optical coherence tomography

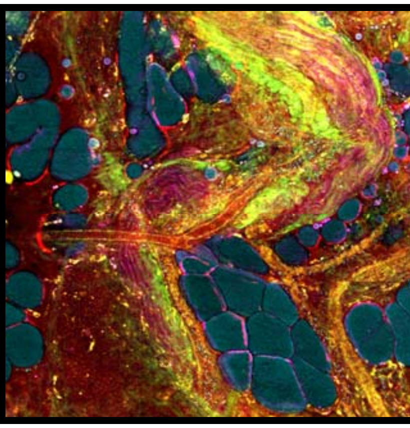

Biomedical Imaging

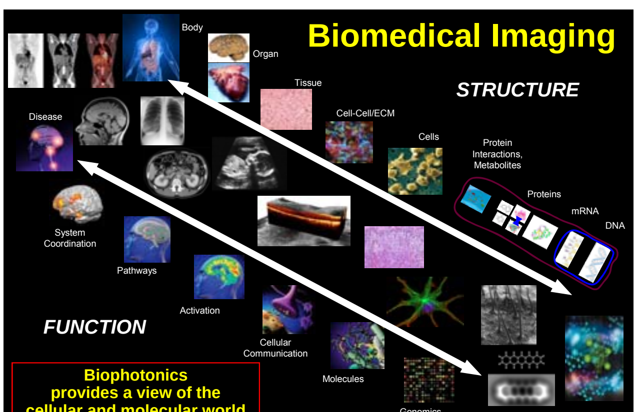

Biophotonics provides a view of the cellular and molecular world

Optical Coherence Tomography (OCT)

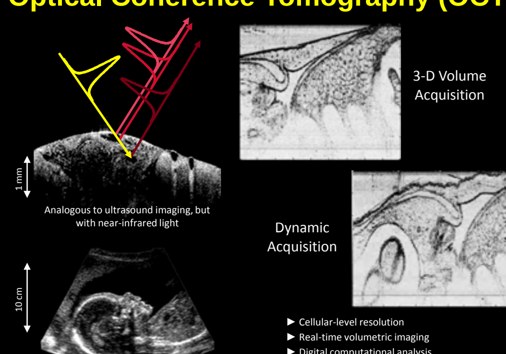

- Cellular-level resolution
- Real-time volumetric imaging
- Digital computational analysis
- Compact and modular optical systems

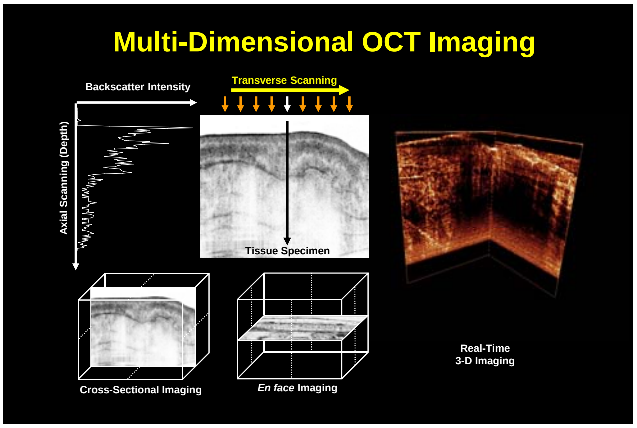

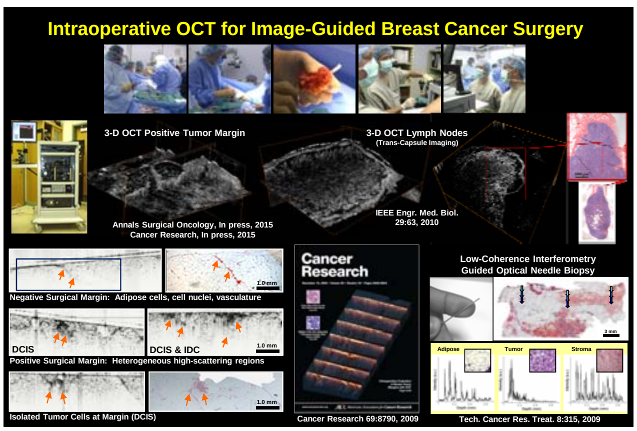

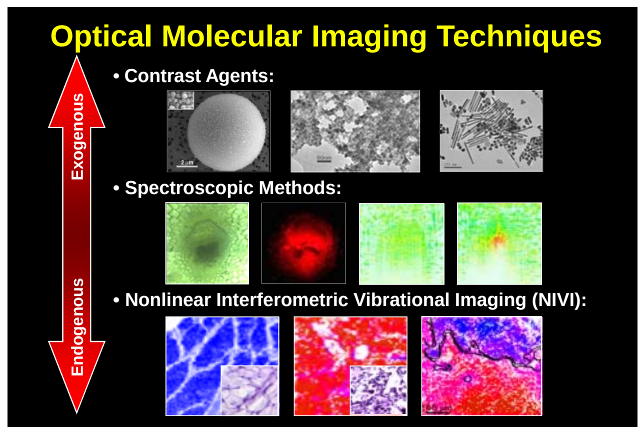

Motivation

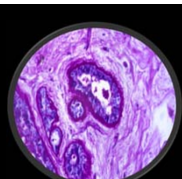

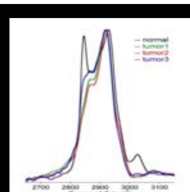

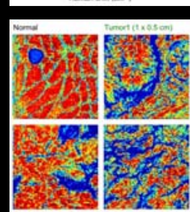

- Stained histopathology is the gold standard, but remains subjective
- New sensitive assays for rapid analysis and quantitative molecular histopathology are needed
- Can we develop label-free optical molecular spectroscopy and imaging technologies that can rapidly and quantitatively diagnose disease?

Optical Scattering Processes for Tissue Diagnosis

Elastic Scattering Processes: ***Reflectance, Structural OCT***

Inelastic Scattering Processes: ***Fluorescence, Spontaneous Raman***

Stimulated Coherent Inelastic Scattering Processes:
Stimulated emission, Stimulated Raman scattering
Four-wave mixing processes, SHG, THG
Coherent Anti-Stokes Raman Scattering (CARS)

- **Coherent Anti-Stokes Raman Scattering (CARS) produces measurable signal with sufficient power**
- **Take advantage of the coherent nature of CARS and use interferometry to provide both amplitude and phase information for molecular diagnostics**

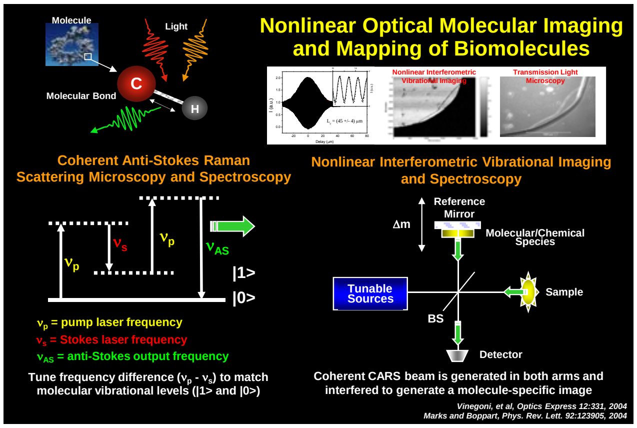
Nonlinear Optical Molecular Imaging and Mapping of Biomolecules
Molecule
Light
Molecular Bond
C
H
Coherent Anti-Stokes Raman Scattering Microscopy and Spectroscopy
Nonlinear Interferometric Vibrational Imaging and Spectroscopy
Nonlinear Interferometric Vibrational Imaging
Transmission Light Microscopy
|1>
|0>
νp = pump laser frequency
νs = Stokes laser frequency
νAS = anti-Stokes output frequency
Tune frequency difference (νp - νs) to match molecular vibrational levels (|1> and |0>)
Reference Mirror
Δm
Molecular/Chemical Species
Tunable Sources
Sample
BS
Detector
Coherent CARS beam is generated in both arms and interfered to generate a molecule-specific image
Vinegoni, et al, Optics Express 12:331, 2004
Marks and Boppart, Phys. Rev. Lett. 92:123905, 2004

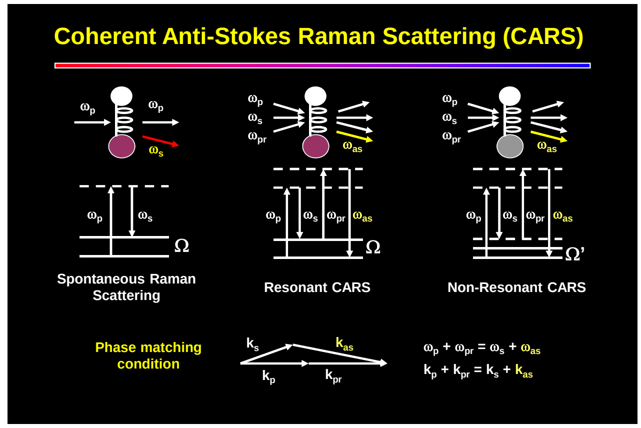
Coherent Anti-Stokes Raman Scattering (CARS)
Spontaneous Raman Scattering
Resonant CARS
Non-Resonant CARS
Ω
Ω'
Phase matching condition
ωp + ωpr = ωs + ωas
kp + kpr = ks + kas

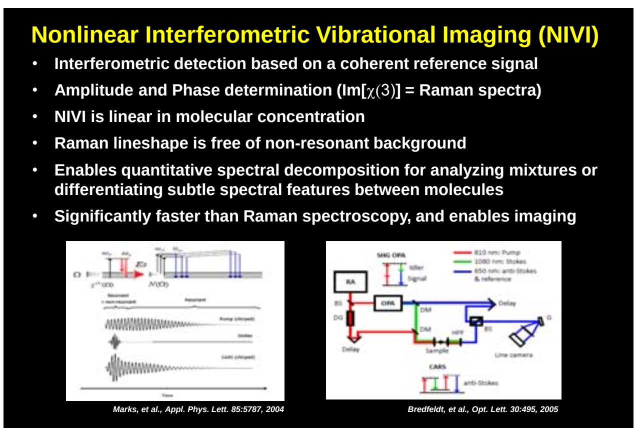
Nonlinear Interferometric Vibrational Imaging (NIVI)
• Interferometric detection based on a coherent reference signal
• Amplitude and Phase determination (Im[χ(3)] = Raman spectra)
• NIVI is linear in molecular concentration
• Raman lineshape is free of non-resonant background
• Enables quantitative spectral decomposition for analyzing mixtures or differentiating subtle spectral features between molecules
• Significantly faster than Raman spectroscopy, and enables imaging
Marks, et al., Appl. Phys. Lett. 85:5787, 2004
Bredfeldt, et al., Opt. Lett. 30:495, 2005

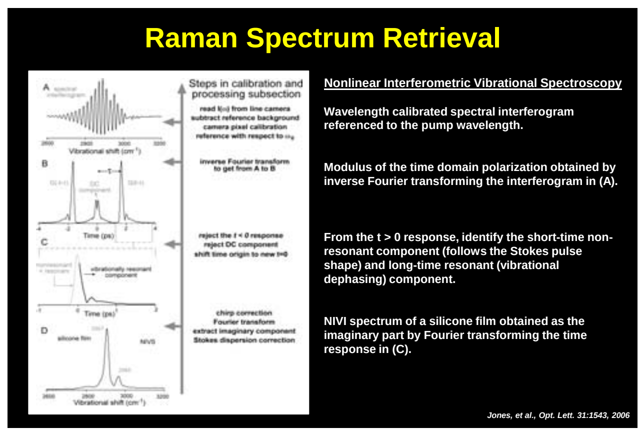
Raman Spectrum Retrieval
Steps in calibration and processing subsection
Nonlinear Interferometric Vibrational Spectroscopy
Wavelength calibrated spectral interferogram referenced to the pump wavelength.
Modulus of the time domain polarization obtained by inverse Fourier transforming the interferogram in (A).
From the t > 0 response, identify the short-time non-resonant component (follows the Stokes pulse shape) and long-time resonant (vibrational dephasing) component.
NIVI spectrum of a silicone film obtained as the imaginary part by Fourier transforming the time response in (C).
Jones, et al., Opt. Lett. 31:1543, 2006

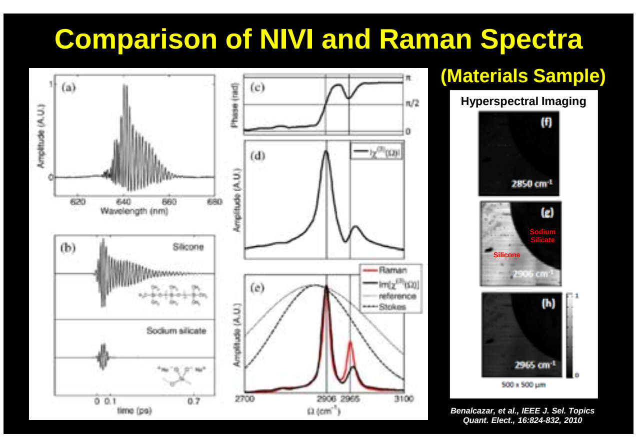
Comparison of NIVI and Raman Spectra
(Materials Sample)
Hyperspectral Imaging
Wavelength (nm)
Silicone
Sodium silicate
time (ps)
Raman
reference
Stokes
Ω (cm⁻¹)
2850 cm⁻¹
2906 cm⁻¹
2965 cm⁻¹
500 x 500 μm
Benalcazar, et al., IEEE J. Sel. Topics Quant. Elect., 16:824-832, 2010

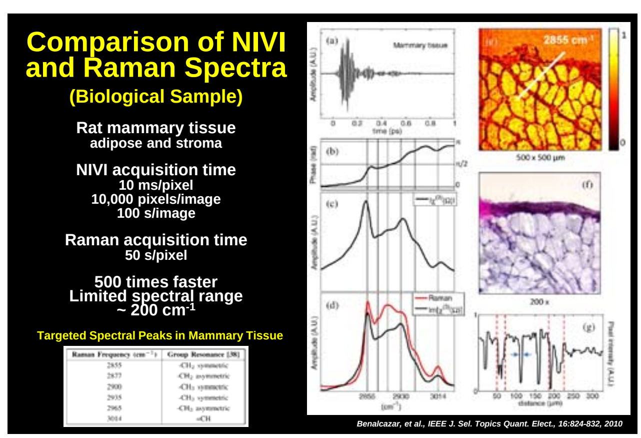
Comparison of NIVI and Raman Spectra
(Biological Sample)
Rat mammary tissue
adipose and stroma
NIVI acquisition time
10 ms/pixel
10,000 pixels/image
100 s/image
Raman acquisition time
50 s/pixel
500 times faster
Limited spectral range
~ 200 cm⁻¹
Targeted Spectral Peaks in Mammary Tissue
Raman Frequency (cm⁻¹)
Group Resonance [38]
2855 cm⁻¹
500 x 500 μm
200 x
Benalcazar, et al., IEEE J. Sel. Topics Quant. Elect., 16:824-832, 2010

Molecular Differentiation using NIVI Spectral Decomposition

Mammary Tissue
(a) Tissue lipids
(b) Tissue proteins
(c) Methyl oleate
(d) Collagen type I

(i) Linear decomposition of basis spectra for (j)
(j) Single point spectrum from NIVI

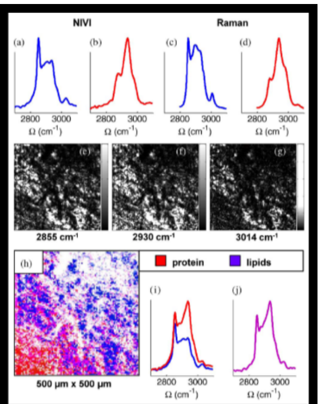

Benalcazar, et al., IEEE J. Sel. Topics Quant. Elect., 16:824-832, 2010

NIVI Cross-Sectional Images of Skin (Porcine)

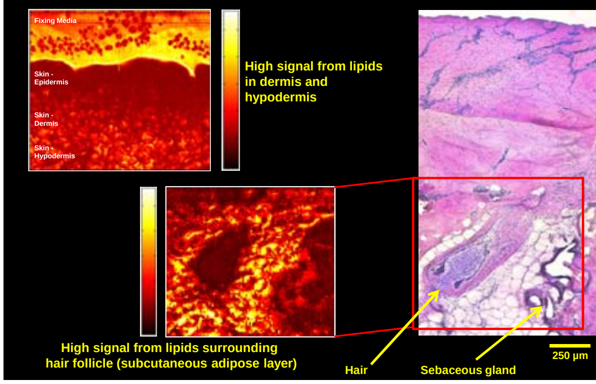

Two main spectral features were observed: Collagen & Lipids

NIVI Image Analysis for Quantitative Molecular Composition

In general, every pixel is a linear superposition of the signals for lipids and collagen

Can obtain the proportion in which both are combined in the resulting signal

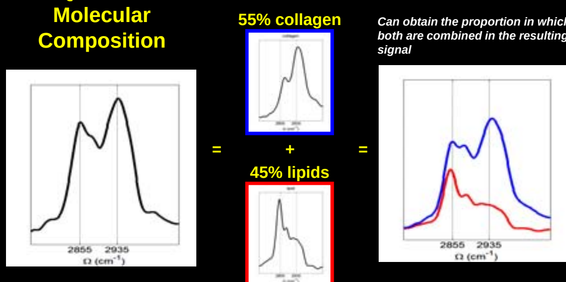

By doing this for each pixel, a quantitative spatial mapping of these two domains is possible

Spectral Identification of Collagen and Lipid Domains

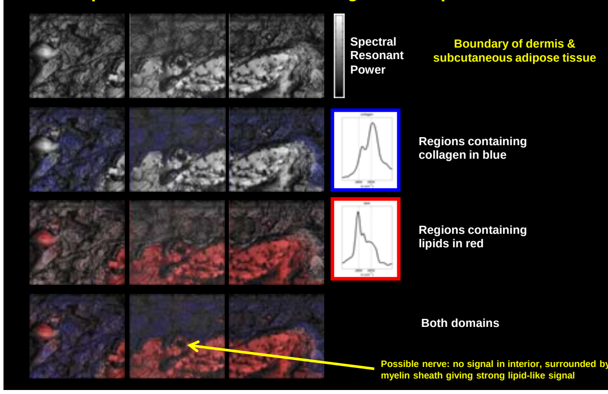

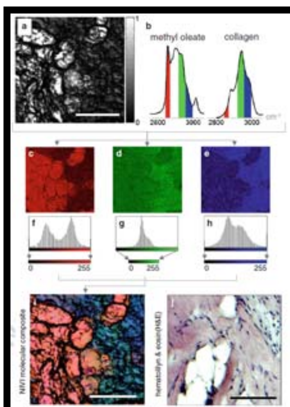

Spectral Decomposition of NIVI Signals from Porcine Skin

j	$\Omega_j - \Omega_{j+1}$ (cm^{-1})	Vibration	Contrast?
1	2,842–2,865	CH_2 symmetric	Yes
2	2,865–2,890	CH_2 anti-symmetric	No
3	2,890–2,913	CH_3 symmetric	No
4	2,913–2,955	CH_3 symmetric	Yes
5	2,955–3,000	CH_3 asymmetric	Yes

Benalcazar and Boppart, Analytical and Bioanalytical Chemistry, 400:2817-2825, 2011

Spectral Decomposition of NIVI Signals from Skin

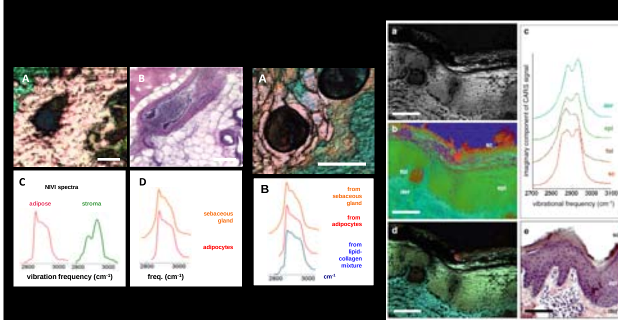

Benalcazar and Boppart, Analytical and Bioanalytical Chemistry, 400:2817-2825, 2011

High-Speed Nonlinear Interferometric Vibrational Analysis of Lipids by Spectral Decomposition

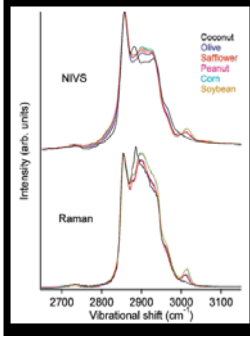

Table 1. Iodine Assay Gives the Number of C=C bonds per Milliliters of Oil ($N_{c=c}$/mL), Which Are Used to Calculate the Average Number of C=C Bonds Per Fatty Acid ($N_{c=c}$/FA) in the Oil[a]

veg. oil	$N_{c=c}$/mL I_2 assay ÷ 1.44×10^{21}	saturated	oleic 1(C=C)	linoleic 2(C=C)	α-linolenic 3(C=C)	$N_{c=c}$/FA calcd	$N_{c=c}$/FA I_2 assay
coconut	0.18	91	6	2		0.10	0.11
olive	1.00	16	71	10	1	0.91	0.76
safflower	1.06	7	78	15		1.08	0.80
peanut	1.25	13	49	32		1.22	0.95
corn	1.89	13	28	58	1	1.47	1.43
soybean	1.92	15	24	54	7	1.53	1.45

[a] Also shown are the approximate % compositions of saturated and unsaturated fatty acids in the different oils. The values of $N_{c=c}$/FA calculated from the % fatty acid compositions is given for comparison.

Table 2. Vibrational Peaks (in cm^{-1}) and Assignments of Unsaturated Fatty Acid Esters[19]

methyl oleate	methyl linoleate	methyl α-linoletae	vibrational assignments
3003	3012	3015	=C−H stretch
2960	2951	2951	C−H stretch (−CH_3 asym)
2929	2924	2935	C−H stretch (−CH_3 sym)
2897	2903	2911	C−H stretch (−CH_3 sym)
2876	2877	2880	C−H stretch (−CH_2 asym)
2856	2855	2855	C−H stretch (−CH_2 sym)
2734	2732	2729	

Chowdary, et al., Analytical Chemistry, 82:3812-3818, 2010

High-Speed Nonlinear Interferometric Vibrational Analysis of Lipids by Spectral Decomposition

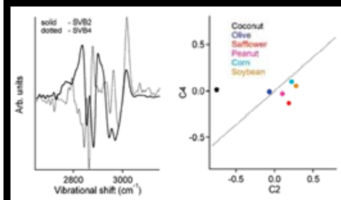

Singular value basis functions with significant contributions to vibrational peak at 3010 cm^{-1}.

Dotted line best represents degree of unsaturation in the oils ($N_{c\text{-}c}$/mL).

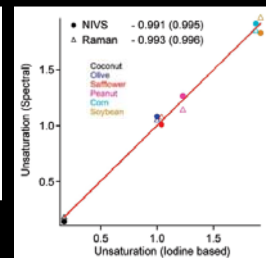

Relative $N_{c\text{-}c}$/mL derived from NIV and Raman spectra plotted against iodine assay.

Values are with respect to $N_{c\text{-}c}$/mL for olive oil (1.44×10^{21}).

Chowdary, et al., Analytical Chemistry, 82:3812-3818, 2010

Quantitative Molecular Histopathology by Spectrally-Resolved NIVI

Biological Pre-Clinical Tumor Model

- **Carcinogen-induced rat mammary tumor model (replicates human DCIS)**
- **At 12 weeks, animals euthanized, mammary tumors removed, flash-frozen, fresh tissue used**
- **Sectioned for NIVI and standard hematoxylin and eosin (H&E) histopathology**
- **Two normal control animals (6 tissue specimens)**
- **Three tumor-bearing animals (13 tissue specimens from 5 different tumors)**

Chowdary, *et al.*, Cancer Research 70:9562, 2010

Quantitative Molecular Histopathology by Spectrally-Resolved NIVI

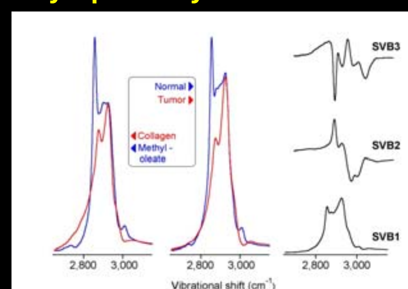

Singular Value Decomposition (SVD) to reduce NIVI data to a few SVD basis spectra

Quantitative Molecular Histopathology

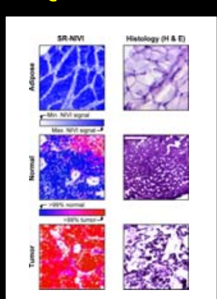

Images 100 x 100 pixels, 500 x 500 μm², 10 ms/pixel

Promising but Challenging for Clinical Translation

Molecular imaging for cancer detection

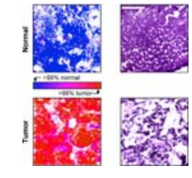

Conventional histology: time-consuming and subjective

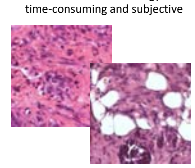

Complex free-space multi-laser system

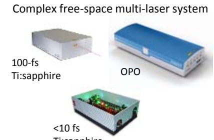

Limited clinical translation

Spectral and Temporal Tailoring of Light

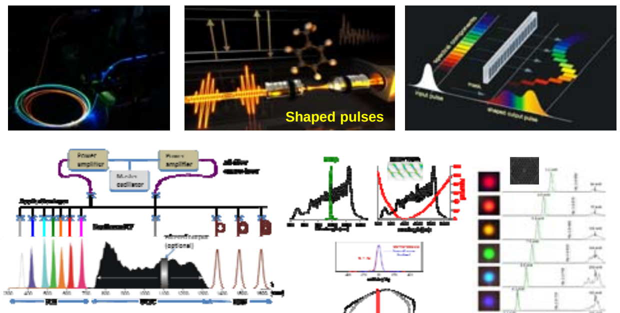

Liu, *et al.*, IEEE J. Sel. Top. Quant. Elect., 18:1209, 2012
Tu and Boppart, Laser & Photonics Reviews, 7:628, 2013
Tu and Boppart, Journal of Biophotonics, 7:9, 2014

Local pulse compression for 2PF, SHG, and THG imaging

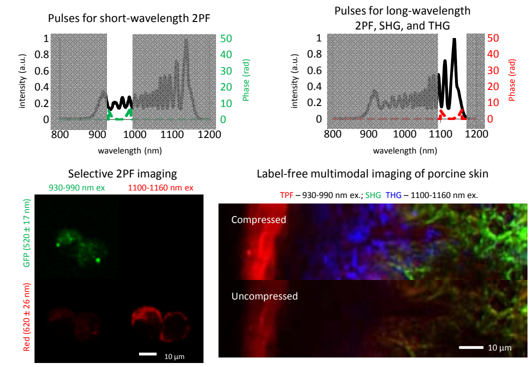

Supercontinuum generation, imaging system, and pulse shaping

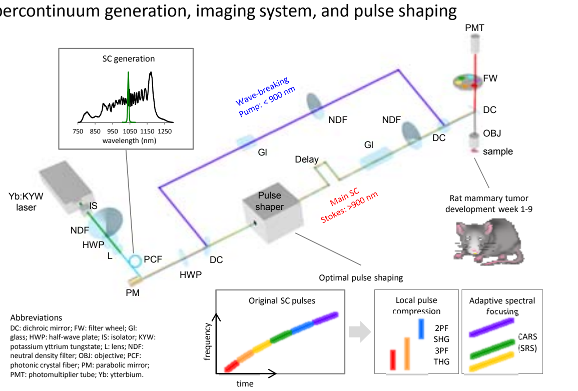

Programmable excitation light becomes an electronic variable …not an alignment setting

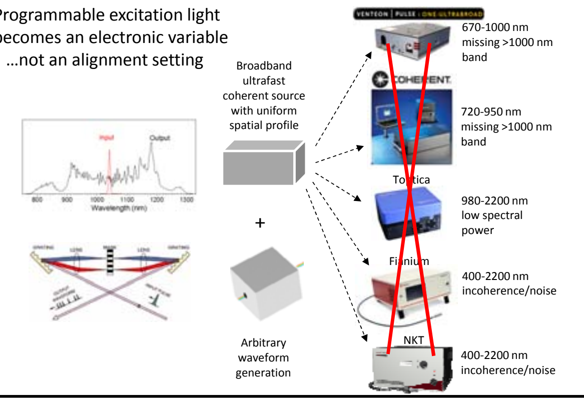

"Coherent" supercontinuum generation by all-normal dispersion photonic crystal fibers

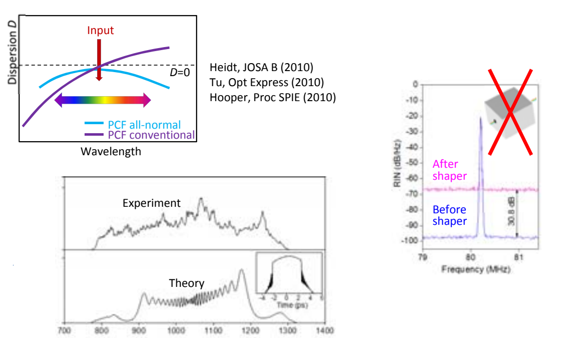

Coherent supercontinuum generation by polarization-maintaining all-normal dispersion photonic crystal fibers

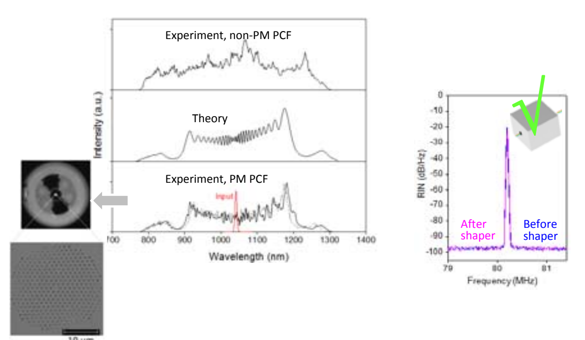

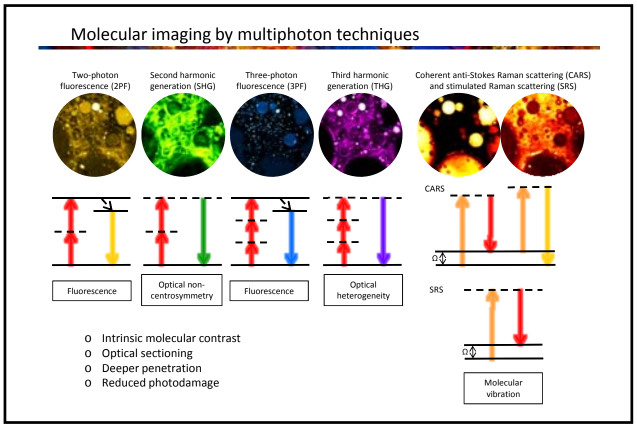
Molecular imaging by multiphoton techniques
Two-photon fluorescence (2PF)
Second harmonic generation (SHG)
Three-photon fluorescence (3PF)
Third harmonic generation (THG)
Coherent anti-Stokes Raman scattering (CARS) and stimulated Raman scattering (SRS)
CARS
SRS
Fluorescence
Optical non-centrosymmetry
Fluorescence
Optical heterogeneity
Molecular vibration
o Intrinsic molecular contrast
o Optical sectioning
o Deeper penetration
o Reduced photodamage

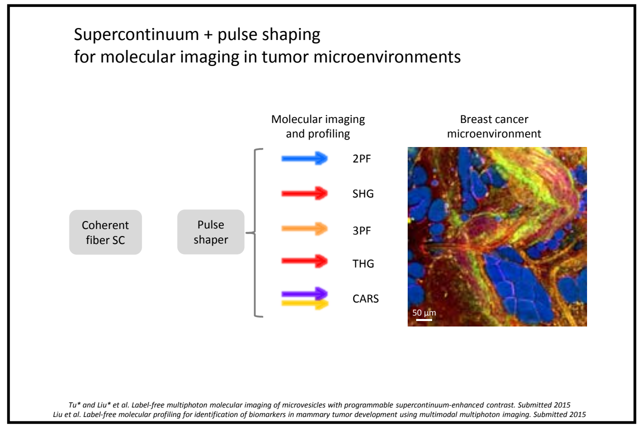
Supercontinuum + pulse shaping
for molecular imaging in tumor microenvironments
Molecular imaging and profiling
Breast cancer microenvironment
Coherent fiber SC
Pulse shaper
2PF
SHG
3PF
THG
CARS
50 µm
Tu* and Liu* et al. Label-free multiphoton molecular imaging of microvesicles with programmable supercontinuum-enhanced contrast. Submitted 2015
Liu et al. Label-free molecular profiling for identification of biomarkers in mammary tumor development using multimodal multiphoton imaging. Submitted 2015

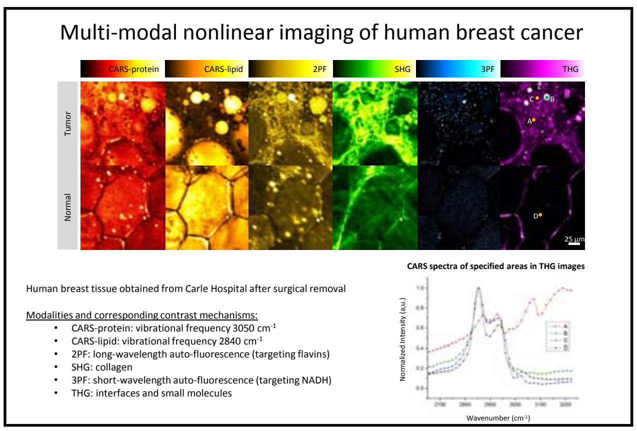
Multi-modal nonlinear imaging of human breast cancer
CARS-protein
CARS-lipid
2PF
SHG
3PF
THG
Tumor
Normal
25 µm
CARS spectra of specified areas in THG images
Normalized Intensity (a.u.)
Wavenumber (cm⁻¹)
Human breast tissue obtained from Carle Hospital after surgical removal
Modalities and corresponding contrast mechanisms:
• CARS-protein: vibrational frequency 3050 cm⁻¹
• CARS-lipid: vibrational frequency 2840 cm⁻¹
• 2PF: long-wavelength auto-fluorescence (targeting flavins)
• SHG: collagen
• 3PF: short-wavelength auto-fluorescence (targeting NADH)
• THG: interfaces and small molecules

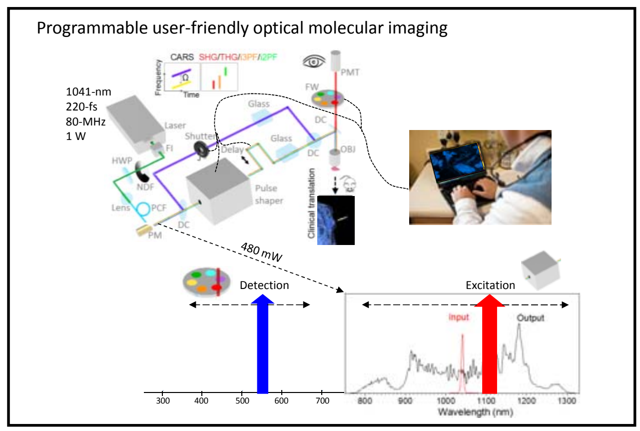
Programmable user-friendly optical molecular imaging
1041-nm
220-fs
80-MHz
1 W
CARS SHG/THG/3PF/2PF
Frequency
Time
PMT
FW
Laser
FI
Shutter
Delay
Glass
Glass
DC
DC
OBJ
HWP
NDF
Lens
PCF
PM
DC
Pulse shaper
Clinical translation
480 mW
Detection
Excitation
Input
Output
300 400 500 600 700 800 900 1000 1100 1200 1300
Wavelength (nm)

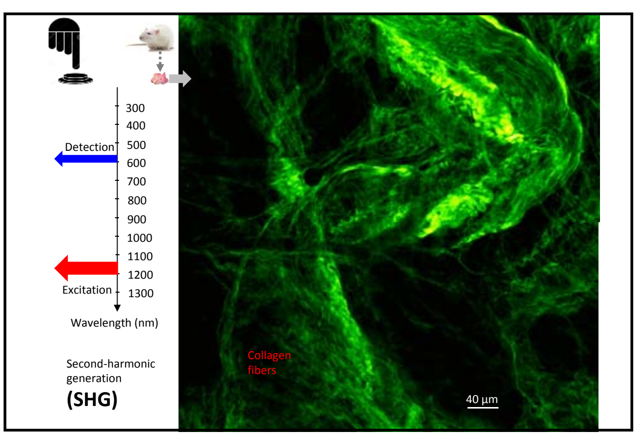
300
400
500
600
700
800
900
1000
1100
1200
1300
Detection
Excitation
Wavelength (nm)
Second-harmonic generation
(SHG)
Collagen fibers
40 µm

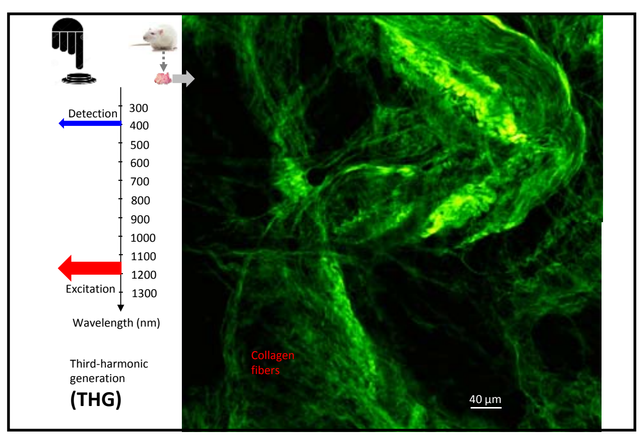
300
400
500
600
700
800
900
1000
1100
1200
1300
Detection
Excitation
Wavelength (nm)
Third-harmonic generation
(THG)
Collagen fibers
40 µm

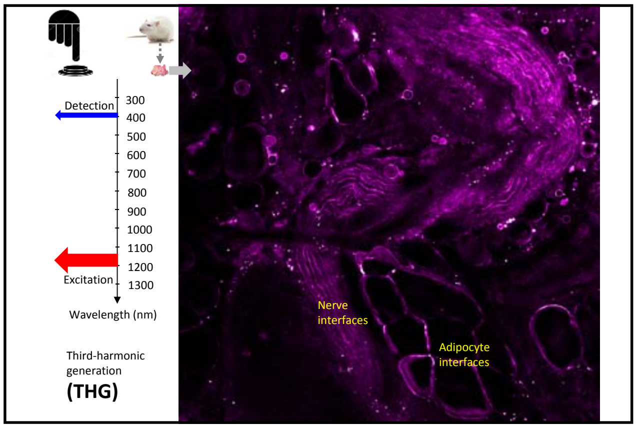
Detection
Excitation
300
400
500
600
700
800
900
1000
1100
1200
1300
Wavelength (nm)
Third-harmonic generation
(THG)
Nerve interfaces
Adipocyte interfaces

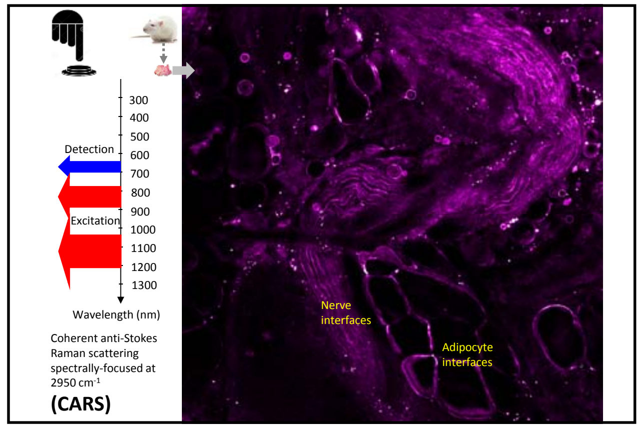
Detection
Excitation
300
400
500
600
700
800
900
1000
1100
1200
1300
Wavelength (nm)
Coherent anti-Stokes Raman scattering spectrally-focused at 2950 cm-1
(CARS)
Nerve interfaces
Adipocyte interfaces

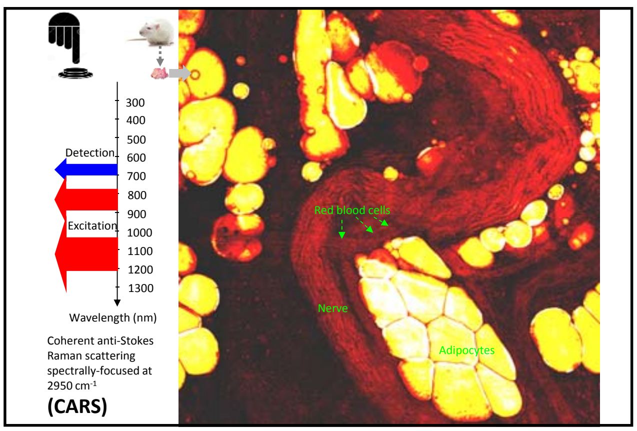
Detection
Excitation
300
400
500
600
700
800
900
1000
1100
1200
1300
Wavelength (nm)
Coherent anti-Stokes Raman scattering spectrally-focused at 2950 cm-1
(CARS)
Red blood cells
Nerve
Adipocytes

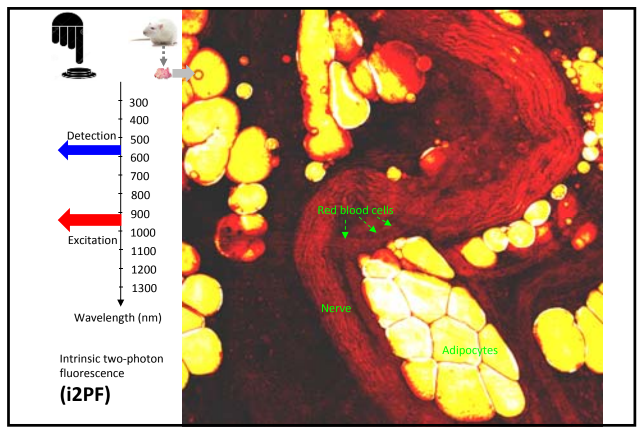
Detection
Excitation
300
400
500
600
700
800
900
1000
1100
1200
1300
Wavelength (nm)
Intrinsic two-photon fluorescence
(i2PF)
Red blood cells
Nerve
Adipocytes

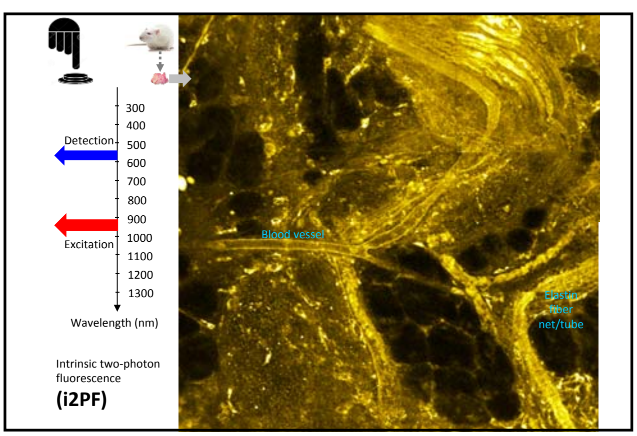
Detection
Excitation
300
400
500
600
700
800
900
1000
1100
1200
1300
Wavelength (nm)
Intrinsic two-photon fluorescence
(i2PF)
Blood vessel
Elastic fiber net/tube

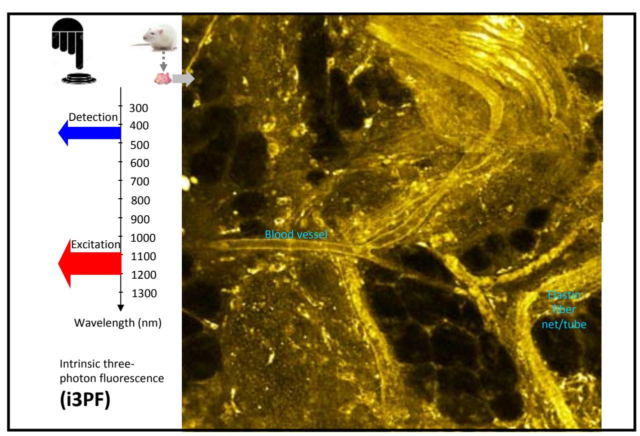
Detection
Excitation
300
400
500
600
700
800
900
1000
1100
1200
1300
Wavelength (nm)
Intrinsic three-photon fluorescence
(i3PF)
Blood vessel
Elastic fiber net/tube

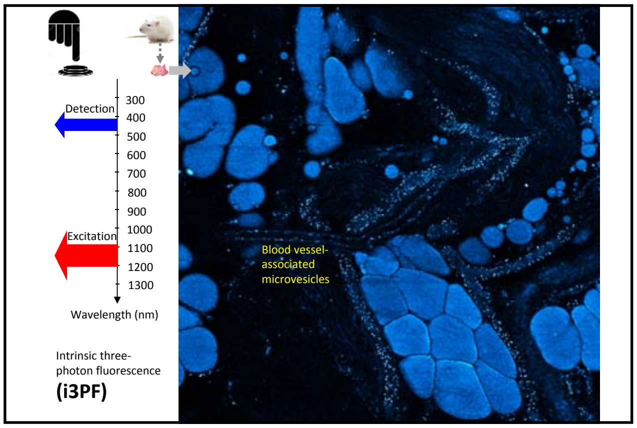

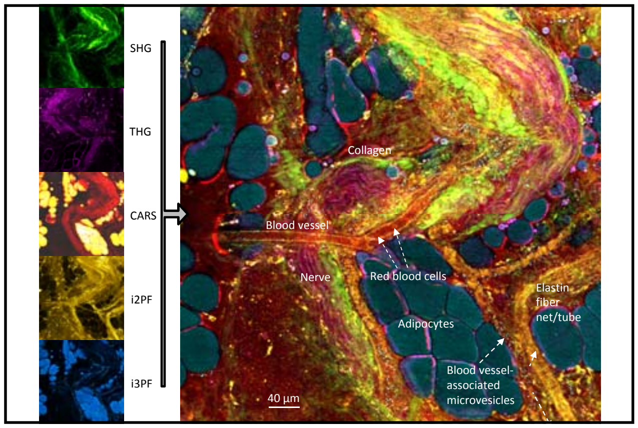

Driving Hypothesis

1. Sparse cancer cells release extracellular vesicles to modulate their microenvironment inside the tissue.
2. Numerous normal cells of the tissue accept the vesicles to switch their metabolism from energy production to biomass production.
3. The switched metabolism induces a structurally modified microenvironment (tumor organ) that promote the proliferation, invasion, and metastasis of the cancer cells.

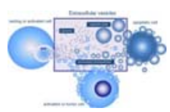
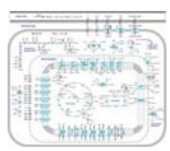
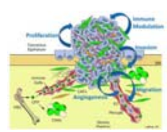

Label-free multimodal multiphoton molecular imaging

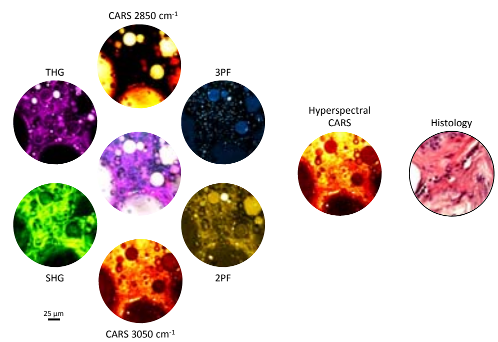

Multiphoton molecular profiling *in situ*

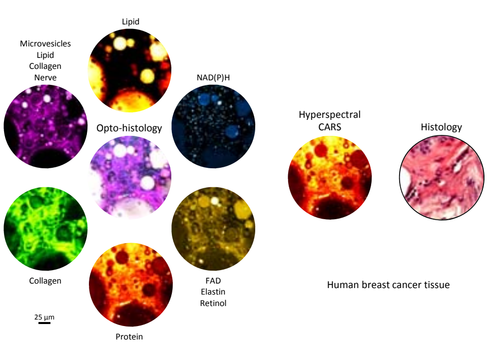

Correlation of multiphoton responses

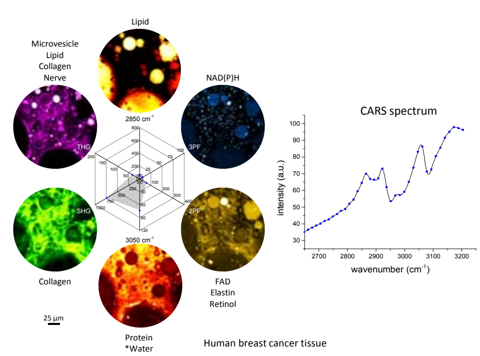

Reading multiphoton molecular profiles

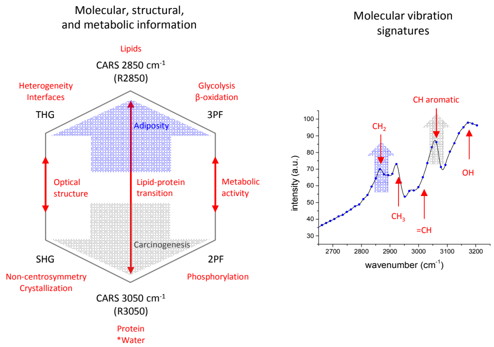

Multiphoton molecular biomarkers in mammary tumor development

Finding multiphoton biomarkers in a carcinogen-induced rat model

- Phenotypic features
- Molecular features
- Correlations and transformations

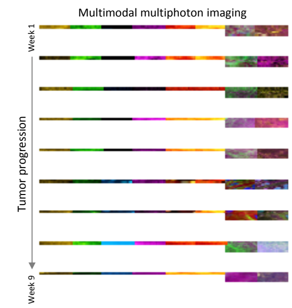

Molecular profiling for mammary tumor development (week 1)

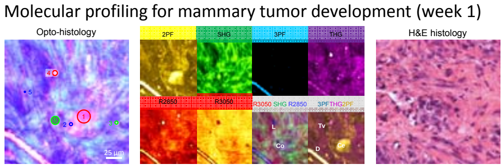

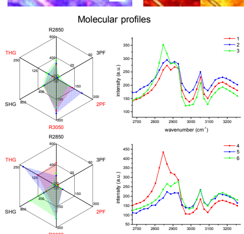

Multiphoton biomarkers
- FAD-fluorescent cell **Ce** (2PF)
- Locally dense collagen **Co** (SHG, THG)
- Tumor-associated THG-sensitive vesicle **Tv** (THG)
- Lipolysis **L** (R2850, THG, 2PF)
- Mammary duct **D** (2PF, 3PF, THG, R2850, R3050)
- CH aromatic stretching vibration (R3050)

Molecular profiling for mammary tumor development (week 3)

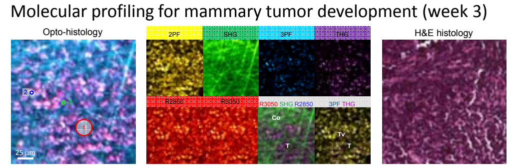

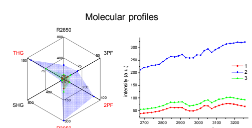

Multiphoton biomarkers
- Tumor cell **T** (2PF, 3PF, THG, R2850, R3050)
- Locally reduced collagen (SHG, THG)
- Tumor-associated THG-sensitive vesicle **Tv** (THG)
- CH aromatic vibration (R3050)

Molecular profiling for mammary tumor development (week 6)

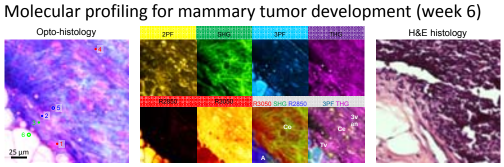

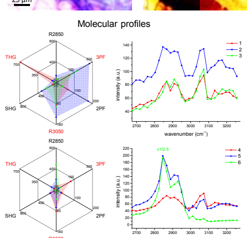

Multiphoton biomarkers
- FAD-fluorescent cell **Ce** (2PF)
- NAD(P)H-fluorescent cell **Ce** (3PF)
- Tumor-associated THG-sensitive vesicle **Tv** (THG)
- Angiogenesis-associated 3PF-sensitive vesicle **3v** (3PF)
- Angiogenesis **an** (3PF, 2PF, SHG, THG, R2850, R3050)
- CH aromatic stretching vibration (R3050)

Molecular profiling for normal mammary tissue (week 6)

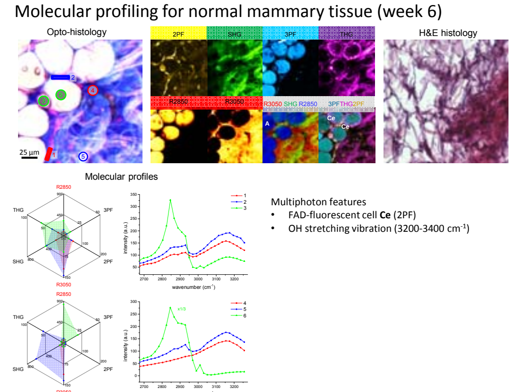

Multiphoton features
- FAD-fluorescent cell **Ce** (2PF)
- OH stretching vibration (3200-3400 cm^{-1})

Molecular profiling for mammary tumor development (week 7)

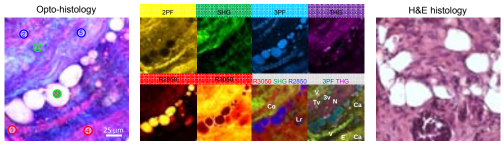

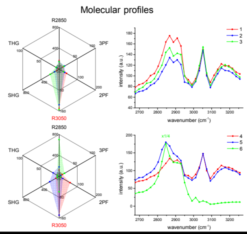

Multiphoton biomarkers

- Elastin organization **E** (2PF)
- Angiogenesis (3PF, 2PF, SHG, THG, R2850, R3050)
- Locally dense collagen (SHG, THG)
- Locally reduced collagen (SHG, THG)
- Tumor-associated THG-sensitive vesicle **Tv** (THG)
- Angiogenesis-associated 3PF-sensitive vesicle **3v** (3PF)
- Blood vessel **V** and capillary **Ca** (2PF, 3PF, SHG)
- CH aromatic stretching vibration (R3050)

Molecular profiling for mammary tumor development (week 9)

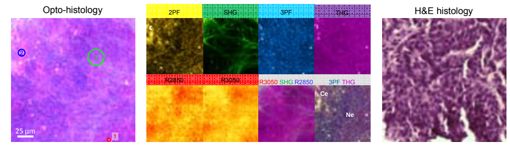

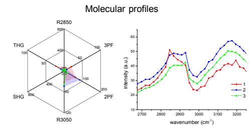

Multiphoton biomarkers

- FAD-fluorescent cell **Ce Ne** (2PF)
- NAD(P)H-fluorescent cell **Ne** (2PF)
- Locally reduced collagen (SHG, THG)
- Tumor-associated THG-sensitive vesicle **Tv** (THG)
- OH stretching vibration (R3200-3400)

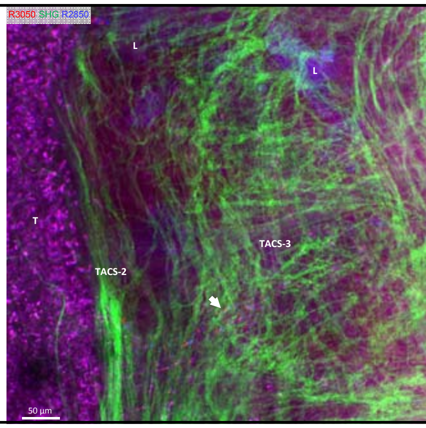

Multiphoton imaging and biomarkers of mammary tumor

Collagen organization
TACS-2: straighten boundary
TACS-3: radially outward
(SHG)

Tumor cell **T** (R2850, R3050)

Lipolysis **L** (R2850)

Local invasion **arrow** (SHG, R2850, R3050)

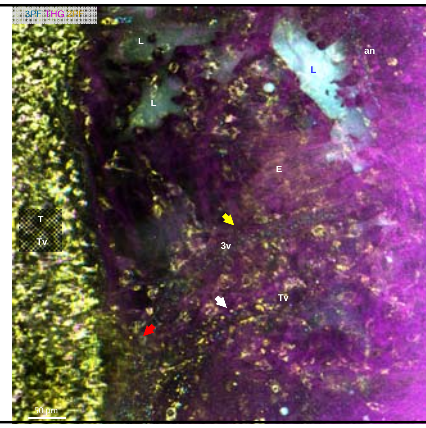

Multiphoton imaging and biomarkers of mammary tumor

FAD-fluorescent cell (2PF)

NAD(P)H-fluorescent cell (3PF)

Tumor cells **T** (2PF, 3PF, THG)

Collagen organization
TACS-2: straighten boundary
TACS-3: radially outward
(THG)

Elastin organization **E** (2PF)

Angiogenesis-associated 3PF-sensitive vesicle **3v** (3PF)

Tumor-associated THG-sensitive vesicle **Tv** (THG)

Lipolysis **L** (3PF, 2PF)

Local invasion **arrows** (2PF, 3PF, THG)

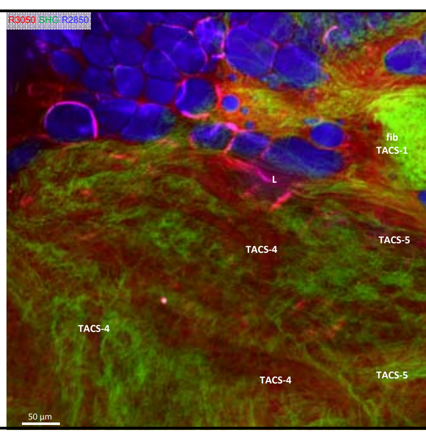

Multiphoton imaging and biomarkers of mammary tumor

Collagen organization
TACS-1: locally dense
TACS-4: locally reduced
TACS-5: tubularly aligned
(SHG)

Fibrocystic change **fib** (SHG)

Lipolysis **L** (R2850, R3050)

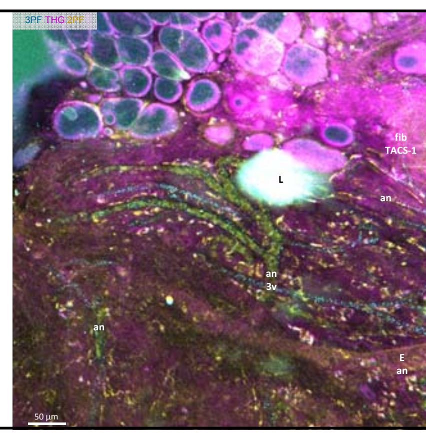

Multiphoton imaging and biomarkers of mammary tumor

FAD-fluorescent cell (2PF)

NAD(P)H-fluorescent cell (3PF)

Collagen organization
TACS-1: locally dense
TACS-4: locally reduced
TACS-5: tubularly aligned
(THG)

Fibrocystic breast **fib** (2PF, THG)

Elastin organization **E** (2PF)

Angiogenesis **an** (3PF, 2PF)

Angiogenesis-associated 3PF-sensitive vesicle **3v** (3PF)

Tumor-associated THG-sensitive vesicle **Tv** (THG)

Lipolysis **L** (3PF, 2PF, THG)

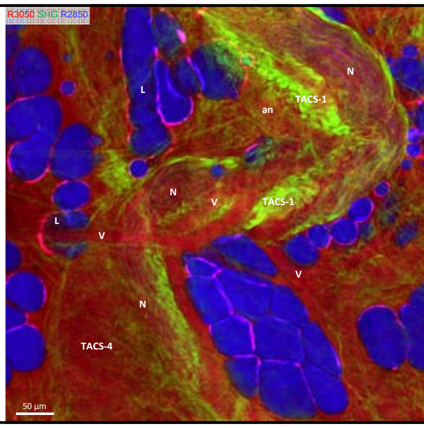

Multiphoton biomarkers in mammary tumor

Collagen organization
TACS-1: locally dense
TACS-4: locally reduced
TACS-5: tubularly aligned (SHG)

Tumor nest **T** (R3050)

Blood vessel **V** (R3050, SHG)

Fibrocystic breast **fib** (SHG)

Lipolysis **L** (R2850, R3050)

Nerve **N** (R2850, R3050)

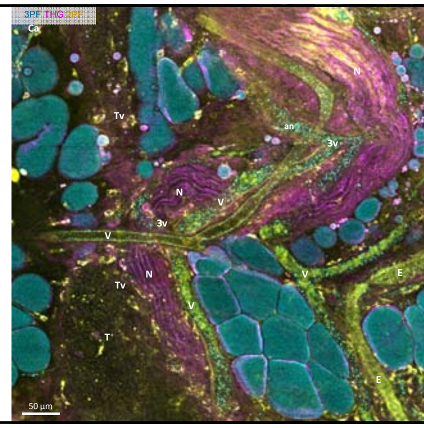

Multiphoton biomarkers in mammary tumor

FAD-fluorescent cell (2PF)

NAD(P)H-fluorescent cell (3PF)

Tumor nest **T** (2PF)

Elastin organization **E** (2PF)

Angiogenesis **an** (3PF, 2PF)

Blood vessel **V** and capillary **Ca** (2PF, 3PF)

Angiogenesis-associated 3PF-sensitive vesicle **3v** (3PF)

Tumor-associated THG-sensitive vesicle **Tv** (THG)

Conclusions

- Broadband coherent fiber light source
- Optimal pulse shaping
- Label-free multi-modal multiphoton imaging and molecular profiling
- Multiphoton cancer biomarkers
- Optical label-free molecular imaging for cancer diagnosis and profiling the tumor microenvironment
- Label-free *in situ* molecular histopathology and surgical guidance

Tu and Liu* el al. Label-free multiphoton molecular imaging of microvesicles with programmable supercontinuum-enhanced contrast. Submitted 2015*

Liu et al. Label-free molecular profiling for identification of biomarkers in mammary tumor development using multimodal multiphoton imaging. Submitted 2015

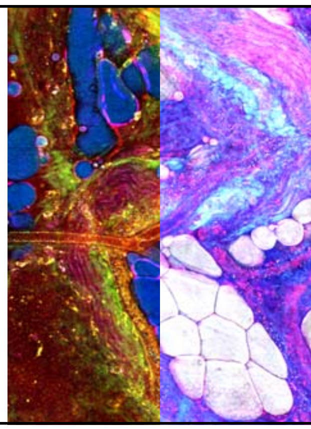

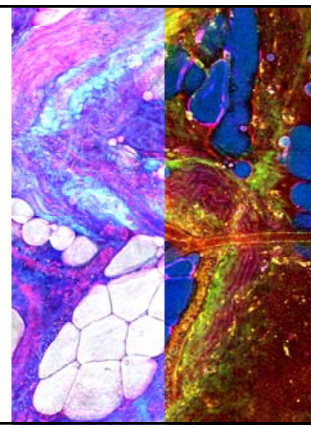

Future Directions

- Fast-scanning, image *in vivo* dynamics
- Developing mathematical formulism to quantify inter-related multimodal changes
- Isolate and characterize microvesicles
- Identify other recurring biomarkers
- Correlate pre-clinical with clinical findings
- Engineer portable system
- Intraoperative imaging during breast cancer surgery
- Investigate pharmacological interventions

Acknowledgments

Beckman Institute
for Advanced Science and Technology
Biophotonics Imaging Laboratory
biophotonics.illinois.edu
Stephen Boppart, M.D., Ph.D.

Graduate Students
Eugene Ark
Andrew Bower, M.S.
Pin-Chieh Huang
Joanne Li, M.S.
Kelly Mesa, M.S.
Guillermo Monroy, M.S.
Fred South, M.S.
Javier Suarez
Sixian You

Undergraduate Students
Shawn Ahn
John Duan
Shravan Gupta
Veronika Sowers

Research Coordinator
Darold Spillman

Research Assistant Professor
Parijat Sengupta, Ph.D.

Post-Docs and Scientists
Eric Chaney
Sarah Erickson-Bhatt, Ph.D.
Marina Marjanovic, Ph.D.
Ryan Nolan, M.S.
Paritosh Pande, Ph.D.
Kush Paul, Ph.D.
Ryan Shelton, Ph.D.
Haohua Tu, Ph.D.
Zhida Xu, Ph.D.
Youbo Zhao, Ph.D.

Academic-Industrial Collaborators:
Dmitry Turchinovich (DTU)
Marcus Dantus (BiophotonicSolutions)
NKT, Inc.

Clinical Collaborators:

Medical Oncology:	Kendrith Rowland, M.D.	Patricia Johnson, M.D., Ph.D.
Surgical Oncology:	Partha Ray, M.D.	Kimberly Craddock, M.D.
	Kelly Cunningham, M.D.	Magesh Sundaram, M.D.
Pathology:	George Liu, M.D.	Krishnan Tangella, M.D.
Otolaryngology:	Michael Novak, M.D.	Ryan Porter, M.D.
Ophthalmology:	Samir I. Sayegh, M.D., Ph.D.	Leanne Labriola, D.O.
Critical Care:	Karen White, M.D., Ph.D.	
Adult Medicine:	Gretchen Sperka, M.D.	Nasreen Syed, M.D.
Primary Care - Pediatrics:	Malcolm Hill, M.D.	

INTERNATIONAL YEAR OF LIGHT 2015